bioRxiv preprint doi: https://doi.org/10.1101/2020.05.15.080218; this version posted May 15, 2020. The copyright holder for this preprint (which was not certified by peer review) is the author/funder. All rights reserved. No reuse allowed without permission.

Rumen protozoa shape microbiome composition and metabolic output of fermentation

Ronnie Solomon[a,b], Tanita Wein[c], Bar Levy[ad], Veronica Reiss[a], Tamar Zehavi[b], Ori Furman[b], Elie Jami[a]

Affiliations:[a] Department of Ruminant Science, Institute of Animal Sciences, Agricultural Research Organization, Volcani Center, Rishon LeZion, Israel. [b] Institute of Natural Sciences, Department of Life Sciences, Ben-Gurion University of the Negev, Beersheba, Israel. [c] Institute of Microbiology, Kiel University, Germany. [d] The Mina and Everard Goodman Faculty of Life Sciences, Bar-Ilan University, Ramat Gan, Israel

#Corresponding author: Elie Jami, Agricultural Research Organization - the Volcani Center, 68 HaMaccabim Road, P.O.B 15159 Rishon LeZion 7505101, Israel, telephone: +972 39683021, fax: +972 3-9683751, e-mail: elie@volcani.agri.gov.il

bioRxiv preprint doi: https://doi.org/10.1101/2020.05.15.080218; this version posted May 15, 2020. The copyright holder for this preprint (which was not certified by peer review) is the author/funder. All rights reserved. No reuse allowed without permission.

Abstract

Background

Eukaryotic ciliate protozoa are an integral part of the rumen microbiome where they account for up to half of the microbial biomass. Protozoa are known to reside in tight association with their surrounding prokaryotic community – either as predators or involved in mutualistic interactions. Nonetheless, the extent of the ecological effect of protozoa on the microbial community as well as their effect on the rumen metabolic output remains largely understudied.

Results

Our study shows that ciliate protozoa determine the metabolic output of the rumen microbiome as well as impose ecological effects on the prokaryotic community. By conducting microcosms experiments over time we find that volatile fatty acids and methane production are highly increased in the presence of protozoa. Analyzing the structure of the prokaryotic community in the presence of protozoa shows that predation enables several species to colonize previously occupied ecological niches. Furthermore, we observe specificity in predation-resistant species across all treatments, while predation susceptible species depends mainly on the source environment. Our results suggest that ecological models describing predation dynamics are applicable when studying host-associated communities.

Conclusions

We conclude that protozoa have a large impact on the rumen ecosystem structure that may determine the overall rumen productivity. Our study further provides insights into natural dynamics as well as the multifaceted role of microbial eukaryotes in host-associated habitats. Thus, when studying the rumen microbial ecosystem, cross-domain interactions between protozoa and prokarya need to be taken into consideration.

bioRxiv preprint doi: https://doi.org/10.1101/2020.05.15.080218; this version posted May 15, 2020. The copyright holder for this preprint (which was not certified by peer review) is the author/funder. All rights reserved. No reuse allowed without permission.

Background

Ruminants represent the hallmark of host-microbe association, as their nutrition almost exclusively relies on the microbial conversion of ingested plant material into consumable products [1]. This process is performed by the highly complex microbial community residing in the first compartment of their digestive tract; the rumen. Accordingly, ruminant productivity is tightly linked with the rumen microbial community composition [2–5]. Several factors are known to impact the ruminal community including colonization history, diet, and host genotype [6–9]. Next to the tight interaction with their host, a complex network of intrinsic interactions shape the host-associated microbial community including symbioses, cross-feeding, antagonisms, competition, and predation [10–14]. Consequently, alterations in these interactions have the potential to greatly affect the ecosystem of the host-associated community, and subsequently host physiology and productivity. While the impact of interactions between prokaryotic species in the rumen gained considerable attention in recent years [11,12,15], the eukaryotic part of the rumen remains largely understudied.

Microbial eukaryotes are known to play a pivotal role in regulating microbial community structure and function as well as physicochemical properties in their habitats [16–18]. Protist-bacteria interactions range from mutualistic (e.g. metabolic exchange or scavenging of toxic compounds [19,20]), to antagonistic interplay that mainly comprises predation [18–20]. Top-down control via predation is thought to be the main cause of bacterial mortality in microbial ecosystems, and was shown to greatly impact community structure, composition and even affecting bacterial morphology and evolution [18]. Bactivorous predation can be broadly divided into specialist and generalist predatory strategies. Predation by generalists leads to a decrease in bacterial abundance and biomass, while a similar compositional distribution is maintained across the prey community [21–23]. In contrast, selective predation affects the relative abundance of a subset of bacterial species potentially leading to a competitive advantage of predation resistant populations [21,24]. Thus, cross-domain interactions between protists and bacteria have the potential to affect the ecological dynamics of microbial communities.

The rumen is not only host to prokaryotes species, but encompasses a diverse community of microbial eukaryotes [14,25]. Ciliate protozoa are considered the dominant eukaryotes in the rumen and account for up to 50% of the total microbial biomass [14,25]. In recent years, most research used a defaunation approach to study the impact of protozoa on the rumen physiology *in-*

bioRxiv preprint doi: https://doi.org/10.1101/2020.05.15.080218; this version posted May 15, 2020. The copyright holder for this preprint (which was not certified by peer review) is the author/funder. All rights reserved. No reuse allowed without permission.

vivo. Defaunation describes the removal of the protozoa population by means of chemical, anti-protozoa compounds or rumen washing [26]. These experiments showed that the *in-vivo* removal of protozoa from the rumen decreased the metabolic end-products of fermentation such as methane and volatile fatty acids (VFAs) [14]. The decrease in methane is likely explained by the mutualistic association of the hydrogen-producing protozoa with the hydrogen-utilizing methanogenic population [27–29]. In addition, *in-vivo* protozoa removal increased the overall nitrogen availability for the animal. The increased nitrogen availability in defaunated animals was suggested to be the result of the absence of predation that allows the digestion of bacteria by the cows in the abomasum, which represents the majority of the nitrogen requirement for the cow [30]. Overall, rumen protozoa are likely to have a diverse predatory nature; for example, Gutierrez (1958) observed that *Isotricha prostoma* ingested specific bacteria while other species were not ingested [31]. In contrast Coleman (1964), observed that *Entodinium caudatum* had no preference in bacterial prey when offered bacterial mixtures with differing proportions [32]. Nonetheless, the impact of protozoa-prokaryote interactions on the rumen microbiome structure and metabolic output remains largely overlooked.

Here we investigate the effect of rumen protozoa on the microbial ecosystem of the rumen. We hypothesize that rumen protozoa play a vital role in determining ecological parameters (e.g., niche availability), and by that, shape microbiome structure and rumen metabolism. To study the ecological consequences of protozoa on the microbial community, we conducted microcosm experiments in which we expose the prokaryotic community to distinct protozoa populations. We characterize the resulting metabolic output and the microbial community composition over time.

Results

Ciliate protozoa increase the metabolic output of the rumen microbiome

To study the effect of protozoa on the metabolic output of the microbial community of the cow rumen, we conducted a microcosm experiment. The experiment was initiated by sampling the rumen fluid of three cows that were kept under the same diet. The protozoa population was separated from the prokaryotic community via sedimentation in a funnel, which was followed by low speed centrifugation at 500xg. After the separation, the protozoa cells were quantified using light microscopy. A total number of 10^4/ml (10^5 overall in 10 ml medium) protozoa cells were used in all microcosm experiments. The microcosms comprised the rumen prokaryotic community

bioRxiv preprint doi: https://doi.org/10.1101/2020.05.15.080218; this version posted May 15, 2020. The copyright holder for this preprint (which was not certified by peer review) is the author/funder. All rights reserved. No reuse allowed without permission.

incubated without protozoa (hereafter referred to as 'protozoa-free' microcosm) and microcosms with the reintroduced protozoa community (Fig. 1a). The microcosms were incubated for 48 h with constant shaking, while methane and volatile fatty acid (VFA) production was quantified after 24 and 48 h. The results of the experiment show that protozoa have a significant effect on the metabolic output of the rumen microbial community (Fig. 1b). In the presence of protozoa, VFA production (the sum of all VFAs) was marginally higher after 24 h than when compared to protozoa-free microcosms (Wilcoxon rank sum, $P = 0.069$; Fig. 1b). We observed a strong effect of the microbial community origin (i.e., source animal) after 24 h that is expected when analyzing metabolic output across individual animals [2] Notably, after 48 h, the sample origin effect subsided and the protozoa effect on metabolic output was more appreciable than after 24 h. While after 48 h the metabolic output generally decreased, the elevated production of VFAs in the presence of protozoa remained consistent across all metabolites (Fig.1b).

Acetate, butyrate, iso-butyrate and iso-valerate were significantly higher in microcosms incubated with the protozoa population (FDR corrected Wilcoxon test $P < 0.05$; Fig. 1b). Notably, acetate and butyrate mainly drove the increase in total VFA with a 12% and 37% increase, respectively, in the protozoa inoculated microcosms. Isovalerate and isobutyrate exhibited the largest fold difference with an average fold increase of 2.5 (150% increase) and 1.7 (74% increase), respectively (Fig. 1b). In addition to the elevated VFA production, the presence of protozoa significantly increased methane emission in the microcosms with a fold increase ranging between x2.5 and x3.5 after 24 h (Wilcoxon test $P < 0.05$; Fig. 1b). The increased methane production in protozoa-inoculated microcosms was maintained after 48 h across all cows. Our results demonstrate that the presence of protozoa in the rumen microbial community greatly influences the production of microbial end-products of the microbiome resulting in higher VFA and methane production.

Protozoa size and identity are important determinants of the metabolic output

The ciliate protozoa population comprises diverse species in the rumen environment [33], that are characterized by different cell sizes ranging between >100 μm to <10 μm. To test whether the size and taxonomic identity of protozoa species differentially influence the VFAs and methane production, the all-protozoa community was fractionated via a series of filtration steps (as previously performed in [27]). Overall, five protozoa fractions were obtained containing different

bioRxiv preprint doi: https://doi.org/10.1101/2020.05.15.080218; this version posted May 15, 2020. The copyright holder for this preprint (which was not certified by peer review) is the author/funder. All rights reserved. No reuse allowed without permission.

protozoa size and taxa (filtersize: 100 µm, 60 µm, 40 µm, 10 µm and filtrate <10; Fig. 1a). The protozoa sub-populations were further characterized using 18s rRNA sequencing (Fig. 1c). The fractions P-100 and F-60, were characterized by large protozoa mainly including *Ophryoscolex* and *Polyplastron* genera, with P-60 also including a large proportion of *Isotricha*. The P-40 fraction was almost exclusively composed of *Isotricha* (93% +/- 4.5). Fractions P-10 and P-<10 were dominated by *Dasytricha*, and to a lesser extent by *Entodinium*. The *Isotricha* genus was detected in all size fractions albeit in different relative abundances (e.g., between 93% in P-40 to 6% in P-<10). The different protozoa populations (i.e., size fractions) were inoculated in separate microcosms containing the whole rumen prokaryotic community of the three cows and incubated for 48 h (Fig. 1a). The production of VFA and methane was measured after 24 h and 48 h.

The results of our experiment reveal that the protozoa populations have a distinct effect on the overall metabolic output of the microbial community (Fig. 1c; Fig S1). The production of VFAs was significantly higher in the large protozoa P-100, P-60 and P-40 populations compared to the small P-10 and P-<10 protozoa populations (Fig. 1c). Notably, the effect of protozoa size and identity was maintained across the microbial source communities and time points. After 48 h, all VFAs, except valerate and propionate, were consistently higher in fractions P-40, P-60 and P-100. Acetate exhibited the strongest size dependence among the VFAs ($R^{2} = 0.37$ $P = 10^{-5}$; Table S1). Interestingly, the P-60 population exhibited the largest variation between the different cows, which may be the result of the intrinsic differences in protozoa distribution compared to the other fractions (Fig. 1c).

In addition, methane production was marginally dependent on the protozoa size fraction, with a higher production in the microcosms with larger protozoa (Linear regression, $R^2 = 0.24$ $P = 0.062$; Table S1). Nonetheless, we observed one protozoa population as outstanding; P-40 produced more methane compared to all other protozoa populations, including P-60 and P-100 (FDR corrected Wilcoxon test $P < 0.01$). The *Isotricha* dominated P-40 fraction exhibited a 1.5-fold higher methane output compared to fractions P-100 and ~3-fold higher compared to the protozoa-free microcosms (Fig. 1b). The methane production in the small protozoa fractions P-10 and F<-10 was significantly lower than in the large protozoa fractions P-40, P-60 and P-100 (FDR corrected Wilcoxon test $P < 0.05$). However, the small protozoa still exhibited a significantly higher methane production compared to the protozoa-free microcosms (Wilcoxon; $P < 0.05$; Fig. S1).

bioRxiv preprint doi: https://doi.org/10.1101/2020.05.15.080218; this version posted May 15, 2020. The copyright holder for this preprint (which was not certified by peer review) is the author/funder. All rights reserved. No reuse allowed without permission.

Our results show that the size of protozoa is a good predictor for the metabolic output of the rumen microbiome, yet, we also demonstrate that protozoa identity may be more important when predicting methane emission.

Large protozoa modulate prokaryotic community ecological structure

Our results so far show that the metabolic output of a rumen microbial community depends not only on the presence of protozoa but also on the specific protozoa group. The observed changes in metabolites may be the result of the protozoa metabolism [34,35], yet might also be the result of alterations induced by the presence of protozoa in the prokaryotic community. To study the potential effect of protozoa on prokaryotic community structure, we analysed the bacteria and archaea composition obtained in all microcosm experiments after 24 and 48 h, via amplicon sequencing of the 16S rRNA in each microcosm. The sequencing of the 16S rRNA yielded 1,024,475 quality reads, with an average of 8,955 ± 2990 reads per sample, which were subsampled to 4800 reads in subsequent analyses. The overall number of Operational Taxonomic Units (OTUs) detected by the analysis was 768, based on ≥97% nt sequence identity between reads.

The results of the sequencing showed that the prokaryotic community composition in the microcosms is to a large extent determined by the environmental context specific to the source environment (i.e., cow individuality, Fig. S2; ANOSIM R= 0.98, $P < 0.0001$), as expected when analysing microbiomes across individual animals or habitats [36]. Nonetheless, a protozoa-dependent clustering of the microcosms' microbial community was observed by assessing each source community separately using the Bray-Curtis similarity metric (Fig, 2a,b,c). In addition, a clustering depending on the protozoa-fraction was evident in the lower dimensions of a PCOA analysis accounting for 11% of the variance between all samples (PC3 PC4, Fig. 2d; Bray-curtis distance). Both analyses showed that the microbial communities of the larger protozoa populations were more similar to each other than to the communities of the smaller protozoa populations and vice versa (Fig. 2a,b,c,d). For example, the P-100 protozoa microbial community was almost always most similar to the P-60 protozoa community regardless of the source environment (Fig. 2 a,b,c,d). Furthermore, when separately analysing the microbial community of the specific protozoa size fractions (across cows), replicates inoculated with the same protozoa fraction were significantly more similar to each other than between the different protozoa fractions (P = 1e-9 using Wilcoxon test; Fig. 2e). When comparing the Bray-Curtis distance between each protozoa-

bioRxiv preprint doi: https://doi.org/10.1101/2020.05.15.080218; this version posted May 15, 2020. The copyright holder for this preprint (which was not certified by peer review) is the author/funder. All rights reserved. No reuse allowed without permission.

containing microcosms to the protozoa-free microcosms, the larger protozoa fractions, P-100, P-60 and P-40, and the microcosms containing the original unfiltered distribution of protozoa (i.e., all protozoa), exhibited the highest distance to the protozoa-free community as well at the largest variation among different microbial communities (Fig. 2f). In contrast, the microcosms incubated with small protozoa were most similar to the protozoa-free community. This shows that different protozoa species had a distinct effect on the community structure of the microbial populations.

To study the impact of protozoa on the species diversity of the microbial communities, we determined the alpha diversity of the microcosms. The analysis showed that communities incubated with larger protozoa species (P-100, P-60 and P-40) tended to have a slightly lower Shannon diversity than the protozoa-free community, when each cow was observed individually, but were not always consistent across replicates (Fig. S3) after 48 h. The species richness (i.e., number of OTUs) was not significantly different between all treatments and was also most dependent on the source communities (Fig. S3). Analysing the community evenness - a measure of the alpha diversity that measures the degree of similarity in abundances between each OTU is in the environment - showed that it was significantly different between the microbial community of the different protozoa fractions (Kruskal-Wallis test P = 0.0007 ; Fig. S3). The communities incubated with the large P-100, P-60 and P-40 protozoa fractions had overall a lower community evenness than the small P-10 and P-<10 protozoa fractions as well as the protozoa-free community after 48 h (Wilcoxon rank sum $P < 0.05$; Fig. S3).

Our results thus show that the presence of distinct protozoa populations had an impact on the microbial communities, with larger protozoa populations inducing the strongest alterations in the microbial community structure compared to the protozoa-free community.

Protozoa enrich for specific bacterial lineages

To quantify the effect of protozoa on the abundance of specific prokaryotic species, we analysed the taxonomic distribution of prokaryotes across all samples. This yielded 14 classes, 26 families, and 31 genera that were present above 0.5% of the total prokaryotic community in at least one of the samples and represented between 85% to 97% of the total prokaryotic community. The result of the taxonomic analysis revealed that several prokaryotic taxa were consistently enriched in microcosms containing protozoa compared to the protozoa-free microcosms, regardless of the source prokaryotic community (Fig. 3; Fig. S4). Comparing the species distribution of protozoa-

bioRxiv preprint doi: https://doi.org/10.1101/2020.05.15.080218; this version posted May 15, 2020. The copyright holder for this preprint (which was not certified by peer review) is the author/funder. All rights reserved. No reuse allowed without permission.

free microcosms to the species changes in communities with protozoa, we observed a stark expansion of the *Gammaproteobacteria* class (Fig.3, Fig. S4). Interestingly, the increase in *Gammaproteobacteria* abundance was mainly observed in communities incubated with the large protozoa fractions P-100, P-60, P-40, where the increase ranged between 3-fold to 20-fold higher bacterial abundance (Wilcoxon rank test, $P < 0.05$; Fig. 3d). Communities incubated with the small protozoa fractions F-10 and F-<10 exhibited a marginal increase in *Gammaproteobacteria* abundance (Fig. S5, $P = 0.07$). Depending on the community source environment, bacterial genera enriched within the *Gammaproteobacteria* were *Succinivibrio, Ruminobacter, Acinetobacter* or all together (Fig. 3a-d). These genera represented on average between 1.4% to 30% in the protozoa-containing communities, while they were in either lower abundance or completely absent in the protozoa-free microcosms ranging between 0% to 4.7%, representing between 2 - 20 average fold increase compared to the protozoa-free microcosms (Fig. 3a-d; Fig. S5). The presence of specific protozoa in the prokaryotic community enriched another class, the *Fibrobacteria*, represented exclusively by the *Fibrobacter* genus. *Fibrobacter* was 10-fold higher in abundance in microcosms incubated with the largest F-100 protozoa species (Fig. 3d). Interestingly, while Fibrobacter was undetectable in one source (cow) community, and remained absent in protozoa-free microcosms, it could be observed in the microbial community of the microcosms incubated with protozoa (Fig. 3a). In addition, the genus *Treponema,* of the *Spirochetes* phylum*,* exhibited a significantly higher abundance in microcosms of protozoa fractions F-100 and F-60. Analysing the differential species abundance at the OTU level revealed that several OTUs belonging to *Succinivibrionaceae*, *Treponema*, *Fibrobacter*, *Veillonellaceae* and *Bacteroidales*, were enriched in the presence of protozoa, regardless of the source community, and constituted ~30% of the increasing OTUs (Fig. 3e). This result shows that not only specific genera, but specific OTUs are affected by the presence of protozoa.

Interestingly, the methanogens did not increase in relative abundance in most microbial communities. Only in two communities (P-100 and P-60), stemming from the same cow, *Methanobrevibacter* increased compared to the protozoa-free environment (Fig. 3a). Consequently, the increase in methane emission observed in the presence of protozoa cannot be attributed to the free-living methanogenic community. In contrast to the pattern of increasing taxa, the taxa that decreased in abundance in the presence of protozoa were more diverse across all microcosms (Fig. 3e). In addition, for the decreasing taxa we observed a strong dependence on

bioRxiv preprint doi: https://doi.org/10.1101/2020.05.15.080218; this version posted May 15, 2020. The copyright holder for this preprint (which was not certified by peer review) is the author/funder. All rights reserved. No reuse allowed without permission.

their abundance in the source (original) community. For example, OTUs belonging to *Bacteroidetes* (most abundant genus *Prevotella)* were decreasing in microcosms that exhibited the highest abundance of this phylum in its source community (90% and 80% compared to 56% in the third cow; Fig 3e, Fig. S5). Another example are OTUs from *Firmicutes* that mostly decreased in the microbial community originated from one cow where it was observed in the highest abundance (35% compared to 5% and 4% in the two other cows (Fisher exact test on the distribution of decreasing OTUs across cows; $P < 0.0001$). Notably, a decrease in *Fusobacterium* could be observed in two of the source communities, where it significantly decreased in the large P-100 and P-60 communities (Fig. 3d). Analysing decreasing prokaryotic taxa at the OTU level, we observed only one out of 29 decreasing OTUs that exhibited a consistent decrease compared to the protozoa-free microcosms across all the source environments (i.e., cows). Thus, the shared number of decreasing prokaryotic species was significantly lower than the shared increasing OTUs (Fisher exact test increasing vs. decreasing; $P < 0.001$; Fig 1d).

Overall, our results show that taxa which decreased in the microcosm were more diverse and the decrease in abundance was dependent on the initial context of the microbial community, while the increasing taxa were mainly related to the presence of the specific protozoa population. Thus, we conclude that protozoa have the potential to impose selection on specific prokaryotic species potentially allowing for competitive advantages in the rumen ecosystem.

Discussion

Host-associated microbial communities can be altered by several factors including host species or genetics [7,9,37], host lifestyle such as diet, and geography of the host [8]. However, within the constraint of these parameters, microbiome internal parameters, such as interactions between its species, can shape community structure as well [11]. Our results show that the presence of microbial eukaryotes in microbial communities greatly impacts prokaryotic species composition and abundance. By comparing microbial variation between populations with and without the presence of ciliate protozoa we find that protozoa enable previously rare bacterial groups to thrive in the ecosystem. Hence, rumen protozoa have the potential to provide certain bacterial species with a competitive advantage. This is in line with the keystone predation model [23,38], which predicts that predation susceptible and resistant competitor species can coexist but negative selection by elevated predation in high productivity leads to stronger positive selection for

bioRxiv preprint doi: https://doi.org/10.1101/2020.05.15.080218; this version posted May 15, 2020. The copyright holder for this preprint (which was not certified by peer review) is the author/funder. All rights reserved. No reuse allowed without permission.

predation resistant bacteria, where the competitive niche-opening is filled by the latter. Examples for species involved in such ecological trade-offs between competition and predation include several genera of the *Gammaproteobacteria* that were shown to be predation-resistant against diverse protists in aquatic environments [39,40]. It was further speculated that type III, IV and type VI secretion systems, which are commonly encoded in their genomes, may assist in the observed digestion resistance [39] with type III secretion system also identified in *Gammaproteobacteria* species in the rumen [41]. In our experiment, *Gammaproteobacteria*-associated taxa were significantly enriched in the presence of protozoa, while in several microcosms they became more dominant than the typically prevailing *Bacteroidetes* and *Firmicutes*. Interestingly, within the rumen environment *Gammaproteobacteria* were shown to display a large variability in abundance between cows, even under similar management and diet[42,43]. Therefore, our results offer an explanation to such variations, where protozoa composition and abundance play a role in enriching *Gammaproteobacteria*. Additional evidence for a trade-off between competition and predation is the higher abundance of *Ruminobacter* coupled with a simultaneous decrease in *Streptococcus* and *Prevotella* (depending on the original source environment) in microcosms containing protozoa (Fig. 3). Several species of these genera are known as amylolytic species (e.g., *Ruminobacter Amylophilus*, *Streptococcus Bovis*, and species of *Prevotella* such as *Prevotella Ruminicola, Prevotella Bryantii*)[44], which suggests that *Ruminobacter* has a competitive advantage in the presence of protozoa. Another example of a taxa that may evade predation is *Fibrobacter*; *Fibrobacter succinogenes* was shown to encode a specific glycocalyx coating that enables adherence to plant cell wall and was suggested to protect against engulfment by protozoa [45,46]. The prey range of a protozoa (generalist vs. specialist predation) may change the relative abundance of prokaryotic species. Our results show that most protozoa prefer no specific prey taxa (OTU) but rather a wide breadth of prey species that was strongly dependent on the abundance in the source environment. For example, *Bacteroidetes* decreased across two environments that had the highest original abundance of this phylum and taxa belonging to *Firmicutes* decreased in one cow that exhibited a high abundance in the original microbiome. Nonetheless, our results showed that the community evenness was decreased in the presence of protozoa, which suggests that selective predation by specialist predators allow only predation- resistant taxa to proliferate at the expense of the rest of the prokaryotic community. We propose that predation by protozoa is mostly dependent on the context of the bacterial community in terms of effect on prey while intrinsic

bioRxiv preprint doi: https://doi.org/10.1101/2020.05.15.080218; this version posted May 15, 2020. The copyright holder for this preprint (which was not certified by peer review) is the author/funder. All rights reserved. No reuse allowed without permission.

features of specific bacterial lineages to avoid predation enable their expansion. Our results further suggest that ecological models describing predation dynamics are applicable when studying host-associated communities.

Microbial predation was shown to be an important determinant of ecosystem productivity and functioning [47,48]. Our results suggest that protozoa play a pivotal role in the rumen microbiome end-product output comprising VFAs and methane. A prime example for the effect of predation on productivity is the group of *Succinivibrionaceae* that appeared to be predation resistant in our experiments. *Succinivibrionaceae* were previously associated with higher feed efficiency and lower methane emissions in the rumen [49–51]. Thus, protozoa, in their role as modulator of prokaryotic community composition, may be responsible for differences in production efficiency. Next to their impact on the rumen microbial community, protozoa have on average a larger biomass than prokaryotes. Accordingly, their metabolism may impact the rumen output by a similar scope.

While the higher production of several of the quantified metabolites may be related to the protozoa metabolisms, others such as methane can only be the result of associated methanogens. Several microbial eukaryotes form mutualistic (commensal) relationships with prokaryotes across a wide range of environments [19,52]. Indeed, rumen protozoa were shown to be habitat for a large methanogenic community that is physically associated with the protozoa cells [27–29].

Thus, the elevated methane emission was suggested to be the result of a mutualistic relationship between the hydrogen producing protozoa and the hydrogenotrophic methanogens [14]. Furthermore, the associated methanogen community was shown to represent up to 20% of the total rumen methanogenic community and is suggested to be disproportionately active in terms of methane production with its estimated contribution to methane emission ranging from 10% to 37% [13,53]. Our results are in line with this observation, as the methanogenic rumen community remained largely unchanged across all treatments, a phenomenon further documented in many studies [14,54]. Thus, the strong increase in methane emission measured in the presence of protozoa, is likely explained by the protozoa-associated microbial community.

Conclusion

Many experiments studying the effect of micro-eukaryotic predators on the bacterial community used artificial prey communities comprising a low number of different species or a priorly

bioRxiv preprint doi: https://doi.org/10.1101/2020.05.15.080218; this version posted May 15, 2020. The copyright holder for this preprint (which was not certified by peer review) is the author/funder. All rights reserved. No reuse allowed without permission.

simplified bacterial community [21,48,55]. Our approach allowed us to assess the direct impact of the presence and absence of natural protozoa populations in native prokaryotic communities. Accordingly, our study provides insights into natural dynamics as well as the multifaceted role of microbial eukaryotes in microbial habitats. Protozoa feed on the microbial populations, yet they also provide habitats and nutrients for their surrounding prokaryotes. Thus, when studying the rumen microbial ecosystem, cross-domain interactions between protozoa and prokarya need to be taken into consideration.

Materials and methods

Animal Handling and Sampling

The experimental procedures used in this study were approved by the Faculty Animal Policy and Welfare Committee of the Agricultural Research Organization Volcani Research Center approval no. 737/17 IL, in accordance with the guidelines of the Israel Council for Animal Care.

Rumen fluid was sampled from three cows, while the animals were kept under the same diet (Supplementary Table S1) and transferred immediately to an oxygen free environment in an anaerobic glove box for further processing.

Protozoa separation

In order to obtain different populations of protozoa, the rumen samples underwent a series of size filtration and washings similar to the procedure performed in [27]. Briefly, the rumen fluid was mixed in a 1:1 ratio with warmed, anaerobic Coleman buffer (Williams and Coleman, 2012), and incubated in a separating funnel for 1 h under anaerobic conditions at 39°C. The settled protozoa fraction was transferred to a fresh tube with warm Coleman buffer. Prior to filtration a subset of the whole protozoa community was put aside and represents the all protozoa group in the study. The rest of the protozoa underwent consecutive filtration using nylon net filters (Merck Millipore, Darmstadt, Germany) of different sizes (i.e., 100 µm, 60 µm, 40 µm, 10 µm). The retentate on each filter and the filtrate of the last 10 µm filtering were then washed with a warm anaerobic Coleman buffer [33]. A subset of each fraction was taken for counting under light microscopy in order to be able to inoculate the microcosms with the same number of protozoa. The prokaryotic community was obtained from the upper phase obtained during the protozoa sedimentation process and was

bioRxiv preprint doi: https://doi.org/10.1101/2020.05.15.080218; this version posted May 15, 2020. The copyright holder for this preprint (which was not certified by peer review) is the author/funder. All rights reserved. No reuse allowed without permission.

centrifuge once at 500 ×*g* to remove potential remaining protozoa. Only the upper half of the supernatant was used to minimize contamination of protozoa after centrifugation.

Microcosms preparation

The prokaryotic community was inoculated in 20ml anaerobic screw-cap glass tubes equilibrated in the anaerobic glove box. The rumen fluid containing the prokaryotic community was inoculated with 100mg of ground feed of the same composition the cows received as substrate. The protozoa fractions were centrifuged and concentrated in order to inoculate the microcosms with the smallest amount of volume in order to minimize the carryover of additional ruminal factors that might affect our experiment (150-250 µl, up to 2.5% of the final volume). The overall volume of each microcosm was 10 ml containing 10^4/ml of protozoa from each fraction, and one treatment without protozoa named 'protozoa-free'. The number of protozoa was chosen to reflect the typical abundance of protozoa in the rumen and was also based on a previous experiment showing that this number shows a visible change in methane production (data not shown). The requirement for such protozoa numbers hindered our ability to always obtain the aimed triplicates for all the cows and fractions, thus several groups were performed with two replicates. The microcosms were incubated for 48 h tilted at 30° and shaked at 150 rpm. Methane quantification was performed after 24 h and 48 h. After methane quantification, 5ml of the upper fraction of the microcosms was removed and kept frozen at -80°C for quantification of VFAs and sequencing of the prokaryotic community. The microcosm was complemented with 5 ml of medium M [33], and incubated further for 24 h.

Metabolites quantification

Methane and VFA quantification was performed following the protocol from Shabat et al (2016)[2]. For methane, the incubated samples were removed from incubation and directly placed into the Gas Chromatography (GC) autosampler 10 samples at a time. Samples of 0.250 ml of gas from the headspace of the tubes were injected into a 182.88 cm × 0.3175 cm × 2.1 mm packed Supelco analytical-45/60 Molecular sieve 5 A column (Supelco Inc., Bellefonte, PA, USA) with helium carrier gas set to a flow rate of 10 ml min–1 and an oven temperature of 200 °C. The oven temperature remained steady for a total run time of 5 min. A standard curve was generated using pure methane gas. After the daily measurement 5ml of fluid from each microcosm was removed

bioRxiv preprint doi: https://doi.org/10.1101/2020.05.15.080218; this version posted May 15, 2020. The copyright holder for this preprint (which was not certified by peer review) is the author/funder. All rights reserved. No reuse allowed without permission.

for VFA quantification and microbiome analysis. For VFA measurement, the removed fluid was centrifuged at 10,000g in order to first separate the microbial community from the incubated fluid. The supernatant was transferred to a new tube and the pellet was used for further DNA extraction. 800 µl of the supernatant was mixed with 200 µl of 25% metaphosphoric acid solution (w/v in DDW) followed by 1 min vortex and then incubated at 4 °C for 30 min. The samples were then centrifuged for 15 min at 10,000 g and the supernatant was removed into new tubes, then 250 µl methyl tert-butyl ether (Sigma-Aldrich) was added and the tubes were vortexed for 30 s. Another cycle of centrifugation was performed for 1 min at 10,000 g. The upper phase, which contained methyl tert-butyl ether +SCFAs, was analyzed using an Agilent 7890B GC system (Agilent Technologies, Santa Clara, CA, USA) with a FID detector. The temperatures at the inlet and detector were 250 °C and 300 °C, respectively. Aliquots (1 µl) were injected with a split ratio of 1 : 11 into a 30 m × 0.32 mm × 0.25 µm ZEBRON ZB-FFAP column (Phenomenex, Torrance, CA, USA) with helium carrier gas set to a flow rate of 2.4 ml min–1 and initial oven temperature of 100 °C. The oven temperature was held constant at the initial temperature for 5 min, and thereafter increased at 10 °C min–1 to a final temperature 125 °C, and a final run time of 12.5 min. Individual injections of each pure VFA was performed in order to identify their retention in the column and a calibration curve was generated by preparing an equimolar solution of all the VFA and serially diluting it from 100mM to 0.1mM.

DNA Extraction

DNA extraction was performed as previously described (Stevenson and Weimer, 2007). In brief, cells were lysed by bead disruption using Biospec Mini-Beadbeater-16 (Biospec, Bartlesville, OK, United States) at 3000 RPM for 3 min with phenol followed by phenol/chloroform DNA extraction. The final supernatant was precipitated with 0.6 volume of isopropanol and resuspended overnight in 50–100 µl TE buffer (10 mM Tris-HCl, 1 mM EDTA), then stored at 4°C for short-term use, or archived at -80°C.

Illumina Amplicon Sequencing and Data Analyses

The V4 region of 16S rRNA was amplified by PCR from DNA extracts using barcoded primers 515F 5′-CCTACGGGAGGCAGCAG-3′ and 806rcbR 5′-CCGTCAATTCMTTTRAGT-3′ (Peterson et al., 2009). The barcoded samples were pooled, sequenced in a MiSeq flow cell

bioRxiv preprint doi: https://doi.org/10.1101/2020.05.15.080218; this version posted May 15, 2020. The copyright holder for this preprint (which was not certified by peer review) is the author/funder. All rights reserved. No reuse allowed without permission.

(Illumina) for 251 cycles from one end of the fragment and analyzed with Casava 1.8. Overall 1,024,475 quality reads were obtained, with an average of 8,955 ± 2990 reads per sample.
The Research Laboratory Hylab (Rehovot, Israel) performed amplicon sequencing for the 18S rRNA of the fractionated ruminal samples using primers specifically designed for ciliates taken from Tapio et al. (2016) with the following sequences: CiliF (5′-CGATGGTAGTGTATTGGAC-3′) and CiliR (5′-GGAGCTGGAATTACCGC-3′). Ruminal DNA samples were treated as follows: 20 ng of DNA was used in a 25 µl PCR reaction with primers, using PrimeStar Max DNA Polymerase (Takara) for 20 cycles. The PCR reaction was purified using AmpureXP beads, and then a second PCR was performed using the Fluidigm Access Array primers for Illumina to add the adaptor and index sequences. For this reaction 2 µl of the first PCR were amplified in a 10 µl reaction for 10 cycles. The PCR reaction was purified using AmpureXP beads and the concentrations were measured by Qubit. The samples were pooled, run on a DNA D1000 screentape (Agilent) to check for correct size and for the absence of primer-dimers product. The pool was then sequenced on the Illumina MiSeq, using the MiSeq V2-500 cycles sequencing kit.

Data analysis

Downstream processing of the 16S rDNA data, up to the generation of the OTU table was performed in QIIME v.2 [56]. DADA2 was applied to model and correct Illumina-sequencing amplicon errors [57]. Vsearch was used for the clustering of OTUs based on 97% sequence identity [58]. Taxonomic assignment for the bacterial 16S was performed using the pre-trained classifier Greengenes 13_8 99% OTUs from 515F/806R region from QIIME v.2 pipeline. After the generation of the OTU table, singletons/doubletons were removed and subsampling to an even depth of 4,000 reads per sample was performed for all subsequent analyses. Alpha and Beta diversity analyses were also performed using QIIME v.2 workflow. Principal coordinate analysis (PCOA) using the Bray–Curtis dissimilarity metric based on OTU composition (OTU > 97% identity, species level similarity) were plotted using the PAleontological STatistics software (PAST) (Hammer et al., 2001). Bonferroni corrected analysis of similarity (ANOSIM) was used to test the significance of the group clustering. For most statistical analysis of the compositional differences between the different microcosms groups, unless otherwise stated, Kruskal–Wallis test was used, to assess overall significant differences between the fractions. When Kruskal–Wallis indicated a significant difference between the groups, a *post hoc* Wilcoxon rank sum test was

bioRxiv preprint doi: https://doi.org/10.1101/2020.05.15.080218; this version posted May 15, 2020. The copyright holder for this preprint (which was not certified by peer review) is the author/funder. All rights reserved. No reuse allowed without permission.

performed to determine which paired groups differed from each other. For all the analyses, *P*-values of <0.05 after FDR correction were considered significant, unless otherwise stated in the text or figure. Statistical tests and data analysis across the different fractions were performed in R version 3.5.3. Multiple sequence alignment was performed using MAFFT , using the default parameters. The resulting multiple sequence alignment was used for the reconstruction of a maximum-likelihood phylogenetic tree using IQTree [59], with LG model and 1000 bootstrap replicates. The phylogenetic tree was built using iTOL [60].

Acknowledgments

Our gratitude goes to the ARO farmer and veterinarians for their support throughout this experiment. We want to thank Ido Toyber for his critical reading of the manuscript. We thank Fenna T. Stücker for the graphical design of the experimental scheme.

Funding

This study was supported by grants from the Israeli Dairy Board foundation (Grant No. 362-0524/25) and the Israeli Ministry of Agriculture and Rural Development (Grant No. 362-0542).

Author information

Contributions

EJ and BL conceived the experiment. EJ, RS, BL and VR performed the incubation experiment, metabolite quantification, DNA extraction and sequencing. RS, TZ and OF performed the sequencing. EJ, RS and TW analysed the data. EJ, TW and RS wrote the manuscript. All authors read, revised, and approved the final manuscript.

Ethics declarations

Ethics approval

The experimental procedures used in this study were approved by the Faculty Animal Policy and Welfare Committee of the Agricultural Research Organization Volcani Research Center approval no. 737/17 IL, in accordance with the guidelines of the Israel Council for Animal Care

Consent for publication

Not applicable.

bioRxiv preprint doi: https://doi.org/10.1101/2020.05.15.080218; this version posted May 15, 2020. The copyright holder for this preprint (which was not certified by peer review) is the author/funder. All rights reserved. No reuse allowed without permission.

Conflict of interest

The authors declare that they have no conflict of interest.

References

1. Mackie RI. Mutualistic fermentative digestion in the gastrointestinal tract: diversity and evolution 1. IntegrComp Biol. 2002;42:319–26.

2. Shabat SKB, Sasson G, Doron-Faigenboim A, Durman T, Yaacoby S, Berg Miller ME, et al. Specific microbiome-dependent mechanisms underlie the energy harvest efficiency of ruminants. ISME J. The Author(s); 2016;10:2958.

3. Lima J, Auffret MD, Stewart RD, Dewhurst RJ, Duthie C-A, Snelling TJ, et al. Identification of Rumen Microbial Genes Involved in Pathways Linked to Appetite, Growth, and Feed Conversion Efficiency in Cattle. Front Genet. 2019;10:701.

4. Jami E, White BA, Mizrahi I. Potential role of the bovine rumen microbiome in modulating milk composition and feed efficiency. PLoS One. 2014;9:e85423.

5. Delgado B, Bach A, Guasch I, González C, Elcoso G, Pryce JE, et al. Whole rumen metagenome sequencing allows classifying and predicting feed efficiency and intake levels in cattle. Sci Rep. 2019;9:11.

6. Friedman N, Shriker E, Gold B, Durman T, Zarecki R, Ruppin E, et al. Diet-induced changes of redox potential underlie compositional shifts in the rumen archaeal community. Environ Microbiol. 2016;

7. Wallace RJ, Sasson G, Garnsworthy PC, Tapio I, Gregson E, Bani P, et al. A heritable subset of the core rumen microbiome dictates dairy cow productivity and emissions. Sci Adv. 2019;5:eaav8391.

8. Henderson G, Cox F, Ganesh S, Jonker A, Young W, Collaborators, Global Rumen Census, et al. Rumen microbial community composition varies with diet and host, but a core microbiome is found across a wide geographical range. Sci Rep. 2015;5.

9. Li F, Hitch TCA, Chen Y, Creevey CJ, Guan LL. Comparative metagenomic and metatranscriptomic analyses reveal the breed effect on the rumen microbiome and its associations with feed efficiency in beef cattle. Microbiome. 2019;7:6.

10. Shaani Y, Zehavi T, Eyal S, Miron J, Mizrahi I. Microbiome niche modification drives diurnal rumen community assembly, overpowering individual variability and diet effects. ISME J. 2018;12:2446–57.

11. Moraïs S, Mizrahi I. The Road Not Taken: The Rumen Microbiome, Functional Groups, and Community States. Trends Microbiol. 2019;27:538–49.

bioRxiv preprint doi: https://doi.org/10.1101/2020.05.15.080218; this version posted May 15, 2020. The copyright holder for this preprint (which was not certified by peer review) is the author/funder. All rights reserved. No reuse allowed without permission.

12. Moraïs S, Mizrahi I. Islands in the stream: from individual to communal fiber degradation in the rumen ecosystem. FEMS Microbiol Rev. 2019;43:362–79.

13. Finlay BJ, Esteban G, Clarke KJ, Williams AG, Embley TM, Hirt RP. Some rumen ciliates have endosymbiotic methanogens. FEMS Microbiol Lett. 1994;117:157–61.

14. Newbold CJ, de la Fuente G, Belanche A, Ramos-Morales E, McEwan NR. The role of ciliate protozoa in the rumen. Front Microbiol. 2015;6.

15. Won M-Y, Oyama LB, Courtney SJ, Creevey CJ, Huws SA. Can rumen bacteria communicate to each other? Microbiome. 2020;8:23.

16. Xiong W, Jousset A, Guo S, Karlsson I, Zhao Q, Wu H, et al. Soil protist communities form a dynamic hub in the soil microbiome. ISME J. 2018;12:634–8.

17. Gao Z, Karlsson I, Geisen S, Kowalchuk G, Jousset A. Protists: Puppet Masters of the Rhizosphere Microbiome. Trends Plant Sci. 2019;24:165–76.

18. Pernthaler J. Predation on prokaryotes in the water column and its ecological implications. Nat Rev Microbiol. 2005;3:537–46.

19. Gast RJ, Sanders RW, Caron DA. Ecological strategies of protists and their symbiotic relationships with prokaryotic microbes. Trends Microbiol. 2009;17:563–9.

20. Wein T, Romero Picazo D, Blow F, Woehle C, Jami E, Reusch TBH, et al. Currency, Exchange, and Inheritance in the Evolution of Symbiosis. Trends Microbiol [Internet]. 2019; Available from: http://dx.doi.org/10.1016/j.tim.2019.05.010

21. Bell T, Bonsall MB, Buckling A, Whiteley AS, Goodall T, Griffiths RI. Protists have divergent effects on bacterial diversity along a productivity gradient. Biol Lett. 2010;6:639–42.

22. Johnke J, Baron M, de Leeuw M, Kushmaro A, Jurkevitch E, Harms H, et al. A Generalist Protist Predator Enables Coexistence in Multitrophic Predator-Prey Systems Containing a Phage and the Bacterial Predator Bdellovibrio. Front Ecol Evol. 2017;5:536.

23. Leibold MA. A Graphical Model of Keystone Predators in Food Webs: Trophic Regulation of Abundance, Incidence, and Diversity Patterns in Communities. Am Nat. The University of Chicago Press; 1996;147:784–812.

24. Glücksman E, Bell T, Griffiths RI, Bass D. Closely related protist strains have different grazing impacts on natural bacterial communities. Environ Microbiol. 2010;12:3105–13.

25. Sylvester JT, Karnati SKR, Yu Z, Morrison M, Firkins JL. Development of an assay to quantify rumen ciliate protozoal biomass in cows using real-time PCR. J Nutr. 2004;134:3378–84.

26. Li Z, Deng Q, Liu Y, Yan T, Li F, Cao Y, et al. Dynamics of methanogenesis, ruminal fermentation and fiber digestibility in ruminants following elimination of protozoa: a meta-

bioRxiv preprint doi: https://doi.org/10.1101/2020.05.15.080218; this version posted May 15, 2020. The copyright holder for this preprint (which was not certified by peer review) is the author/funder. All rights reserved. No reuse allowed without permission.

analysis [Internet]. Journal of Animal Science and Biotechnology. 2018. Available from: http://dx.doi.org/10.1186/s40104-018-0305-6

27. Levy B, Jami E. Exploring the prokaryotic community associated within the rumen ciliate protozoa population. Front Microbiol. 2018;9:2526.

28. Ushida K, Newbold CJ, Jouany J-P. Interspecies hydrogen transfer between the rumen ciliate Polyplastron multivesiculatum and Methanosarcina barkeri. J Gen Appl Microbiol. 1997;43:129–31.

29. Lloyd D, Williams AG, Amann R, Hayes AJ, Durrant L, Ralphs JR. Intracellular prokaryotes in rumen ciliate protozoa: Detection by confocal laser scanning microscopy after in situ hybridization with fluorescent 16S rRNA probes. Eur J Protistol. 1996;32:523–31.

30. Storm E, Brown DS, Ørskov ER. The nutritive value of rumen micro-organisms in ruminants: 3. The digestion of microbial amino and nucleic acids in, and losses of endogenous nitrogen from, the small intestine of sheep. Br J Nutr. Cambridge University Press; 1983;50:479–85.

31. Gutierrez J. Observations on Bacterial Feeding by the Rumen Ciliate Isotricha prostoma. J Protozool. 1958;5:122–6.

32. Coleman GS. The metabolism of escherichia coli and other bacteria by entodinium caudatum. J Gen Microbiol. 1964;37:209–23.

33. Williams AG, Coleman GS. The rumen protozoa. Springer Science & Business Media; 2012.

34. Yarlett N, Lloyd D, Williams AG. Butyrate formation from glucose by the rumen protozoon Dasytricha ruminantium. Biochem J. 1985;228:187–92.

35. Ellis JE, McIntyre PS, Saleh M, Williams AG, Lloyd D. Influence of CO2 and low concentrations of O2 on fermentative metabolism of the ruminal ciliate Polyplastron multivesiculatum. Appl Environ Microbiol. 1991;57:1400–7.

36. Bittleston LS, Gralka M, Leventhal GE, Mizrahi I, Cordero OX. Context-dependent dynamics lead to the assembly of functionally distinct microbial communities [Internet]. Nature Communications. 2020. Available from: http://dx.doi.org/10.1038/s41467-020-15169-0

37. Li F, Li C, Chen Y, Liu J, Zhang C, Irving B, et al. Host genetics influence the rumen microbiota and heritable rumen microbial features associate with feed efficiency in cattle. Microbiome. 2019;7:92.

38. Johnke J, Cohen Y, de Leeuw M, Kushmaro A, Jurkevitch E, Chatzinotas A. Multiple micro-predators controlling bacterial communities in the environment. Curr Opin Biotechnol. 2014;27:185–90.

39. Gong J, Qing Y, Zou S, Fu R, Su L, Zhang X, et al. Protist-Bacteria Associations: Gammaproteobacteria and Alphaproteobacteria Are Prevalent as Digestion-Resistant Bacteria in

bioRxiv preprint doi: https://doi.org/10.1101/2020.05.15.080218; this version posted May 15, 2020. The copyright holder for this preprint (which was not certified by peer review) is the author/funder. All rights reserved. No reuse allowed without permission.

Ciliated Protozoa. Front Microbiol. 2016;7:498.

40. Andersson A, Ahlinder J, Mathisen P, Hägglund M, Bäckman S, Nilsson E, et al. Predators and nutrient availability favor protozoa-resisting bacteria in aquatic systems. Sci Rep. 2018;8:8415.

41. Kamke J, Soni P, Li Y, Ganesh S, Kelly WJ, Leahy SC, et al. Gene and transcript abundances of bacterial type III secretion systems from the rumen microbiome are correlated with methane yield in sheep. BMC Res Notes. 2017;10:367.

42. Jami E, Mizrahi I. Composition and similarity of bovine rumen microbiota across individual animals. PLoS One. 2012;7:e33306.

43. Brulc JM, Antonopoulos DA, Miller ME, Wilson MK, Yannarell AC, Dinsdale EA, et al. Gene-centric metagenomics of the fiber-adherent bovine rumen microbiome reveals forage specific glycoside hydrolases. Proc Natl Acad Sci U S A. 2009;106:1948–53.

44. Cotta MA. Amylolytic activity of selected species of ruminal bacteria. Appl Environ Microbiol. 1988;54:772–6.

45. Munn C. Marine microbiology: ecology & applications. Garland Science; 2011.

46. Jun HS, Qi M, Ha JK, Forsberg CW. Fibrobacter succinogenes, a Dominant Fibrolytic Ruminal Bacterium: Transition to the Post Genomic Era. Asian-australas J Anim Sci. Asian-Australasian Association of Animal Production Societies; 2007;20:802–10.

47. Caron DA. Inorganic nutrients, bacteria, and the microbial loop. Microb Ecol. 1994;28:295–8.

48. Saleem M, Fetzer I, Dormann CF, Harms H, Chatzinotas A. Predator richness increases the effect of prey diversity on prey yield. Nat Commun. 2012;3:1305.

49. Wallace RJ, Rooke JA, McKain N, Duthie C-A, Hyslop JJ, Ross DW, et al. The rumen microbial metagenome associated with high methane production in cattle. BMC Genomics. 2015;16:839.

50. Indugu N, Vecchiarelli B, Baker LD, Ferguson JD, Vanamala JKP, Pitta DW. Comparison of rumen bacterial communities in dairy herds of different production. BMC Microbiol. 2017;17:190.

51. Kamke J, Kittelmann S, Soni P, Li Y, Tavendale M, Ganesh S, et al. Rumen metagenome and metatranscriptome analyses of low methane yield sheep reveals a Sharpea-enriched microbiome characterised by lactic acid formation and utilisation. Microbiome. 2016;4:56.

52. Tokura M, Ushida K, Miyazaki K, Kojima Y. Methanogens associated with rumen ciliates. FEMS Microbiol Ecol. Oxford Academic; 1997;22:137–43.

53. Newbold CJ, Lassalas B, Jouany JP. The importance of methanogens associated with ciliate

bioRxiv preprint doi: https://doi.org/10.1101/2020.05.15.080218; this version posted May 15, 2020. The copyright holder for this preprint (which was not certified by peer review) is the author/funder. All rights reserved. No reuse allowed without permission.

protozoa in ruminal methane production in vitro. Lett Appl Microbiol. 1995;21:230–4.

54. Tapio I, Snelling TJ, Strozzi F, Wallace RJ. The ruminal microbiome associated with methane emissions from ruminant livestock. J Anim Sci Biotechnol. 2017;8:7.

55. Karakoç C, Radchuk V, Harms H, Chatzinotas A. Interactions between predation and disturbances shape prey communities. Sci Rep. 2018;8:2968.

56. Bolyen E, Rideout JR, Dillon MR, Bokulich NA, Abnet C, Al-Ghalith GA, et al. QIIME 2: Reproducible, interactive, scalable, and extensible microbiome data science [Internet]. PeerJ Preprints; 2018 Oct. Report No.: e27295v1. Available from: https://peerj.com/preprints/27295/

57. Callahan BJ, McMurdie PJ, Rosen MJ, Han AW, Johnson AJA, Holmes SP. DADA2: High-resolution sample inference from Illumina amplicon data. Nat Methods. 2016;13:581–3.

58. Rognes T, Flouri T, Nichols B, Quince C, Mahé F. VSEARCH: a versatile open source tool for metagenomics. PeerJ. 2016;4:e2584.

59. Chernomor O, von Haeseler A, Minh BQ. Terrace Aware Data Structure for Phylogenomic Inference from Supermatrices. Syst Biol. 2016;65:997–1008.

60. Letunic I, Bork P. Interactive Tree Of Life (iTOL) v4: recent updates and new developments. Nucleic Acids Res. 2019;47:W256–9.

Figures legends

Figure 1. Metabolic output of microcosms incubated with Protozoa. (a) Experimental setup of the microcosm experiments. The rumen microbial community of three cows were sampled and separated from protozoa cells. This was conducted either for all protozoa or according to the protozoa size. Subsequently, the microbial community was incubated with the different protozoa populations. **(b)** Metabolic output of microcosms incubated with and without protozoa. The production of methane and VFAs was measured after 24 h and 48 h in microbial communities that were either protozoa-free or incubated with the total protozoa population (n=2-3 for each cow). **(c)** Production of metabolites of microbial communities incubated with different protozoa-size fractions. Metabolites were measured after 24 h and 48 h in microbial communities from three cows (n=2-3 for each cow) that were incubated with different protozoa-size populations (for original data see Supplementary Fig.S1). Each row is represented by the z-score for each metabolite. Top: Stack bars show the genus level of the protozoa species in the microcosm.

bioRxiv preprint doi: https://doi.org/10.1101/2020.05.15.080218; this version posted May 15, 2020. The copyright holder for this preprint (which was not certified by peer review) is the author/funder. All rights reserved. No reuse allowed without permission.

Figure 2. Ecological structure of the prokaryotic community across microcosms. (a-c) Principal coordinate analysis (PCOA) plot of the microcosms separated by source sample and based on Bray-Curtis similarity metric after 48 h. Analysis of similarity test (ANOSIM) on the overall groups was performed. **(d)** PCOA based on coordinates 3 and 4 (PC3, PC4) of the three cows that reveals a fraction based clustering. **(e)** Bray-Curtis distance within replicates across the microcosms compared to the distance between the replicates. The values used are the individual values obtained for each source (i.e. cow) sample. Wilcoxon rank test was used to test for significance ($P = 10^{-9}$). **(f)** Bray-Curtis distance between the protozoa-free microcosms and microcosms containing different protozoa fractions. Pairwise distance between the microcosms containing different protozoa fractions and the protozoa free microcosms. Wilcoxon rank test was used to test for significance with boxes not sharing a letter significant at $P < 0.05$.

Figure 3. Taxonomic differences between microcosms. (a-c) The relative abundance of the different genera in the microbial communities was square root transformed and is displayed for each cow. The genera are ordered based on their rank abundance in the protozoa-free microcosms. Color coding is based on the fractions added to the prokaryotic community and only genera that were significantly different from the protozoa-free fraction are displayed (FDR corrected *t*-test $P < 0.05$). **(d)** Summary of the fold-differences of taxa that were similarly different across the source (i.e. cow) samples. Color coding is based on the different fractions and only the colored bars exhibited a significant difference to the protozoa-free microcosms (using Wilcoxon rank test ($P < 0.05$)). **(e)** Phylogenetic tree of the OTUs that were above 0.5% relative abundance in at least one group of microcosms. Each OTU is color coded based on their phylum affiliation. The colored boxes above each OTU represent their divergence in abundance in the protozoa containing microcosms compared to the protozoa-free microcosms (red=increasing, purple=decreasing, grey= no significant change). The filled and empty black squares represent the cows in which the difference was observed with filled square denoting that a difference was observed in a specific cow. The stack bars represent the square root transformed average abundance of the OTU across fraction P-100 (red), P-60 (blue), P-40 (green) and protozoa-free (grey).

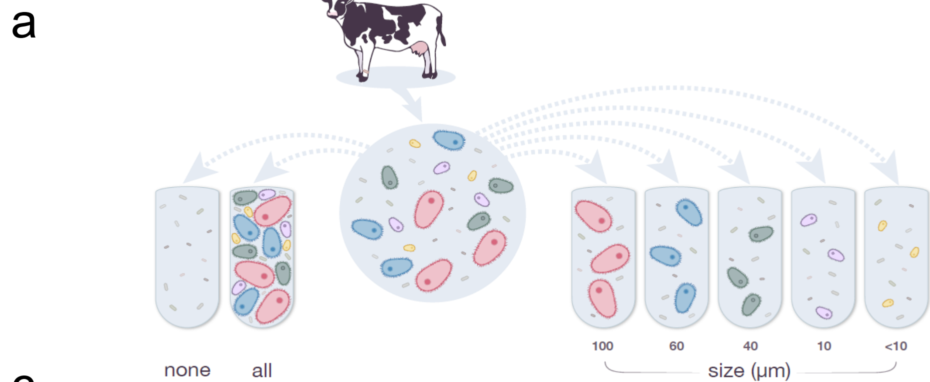
a
none
all
100
60
40
10
<10
size (µm)

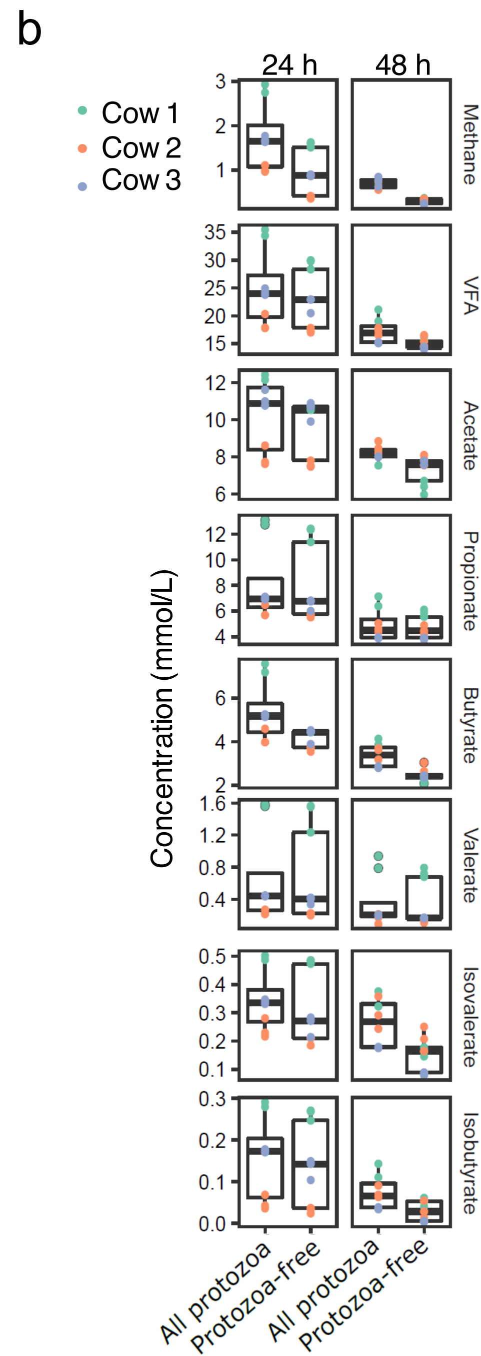
b
24 h
48 h
Cow 1
Cow 2
Cow 3
Methane
VFA
Acetate
Propionate
Butyrate
Valerate
Isovalerate
Isobutyrate
Concentration (mmol/L)
All protozoa
Protozoa-free
All protozoa
Protozoa-free
c
Ophryoscolex
Polyplastron
Isotricha
Dasytricha
Entodinium
Eudiplodinium
Others
No blast hit
Methane
VFA
Acetate
Propionate
Isobutyrate
Butyrate
Isovalerate
Valerate
24 h
48 h
Z-score
P-100
P-60
P-40
P-10
P-<10
Cow 1
Cow 2
Cow 3

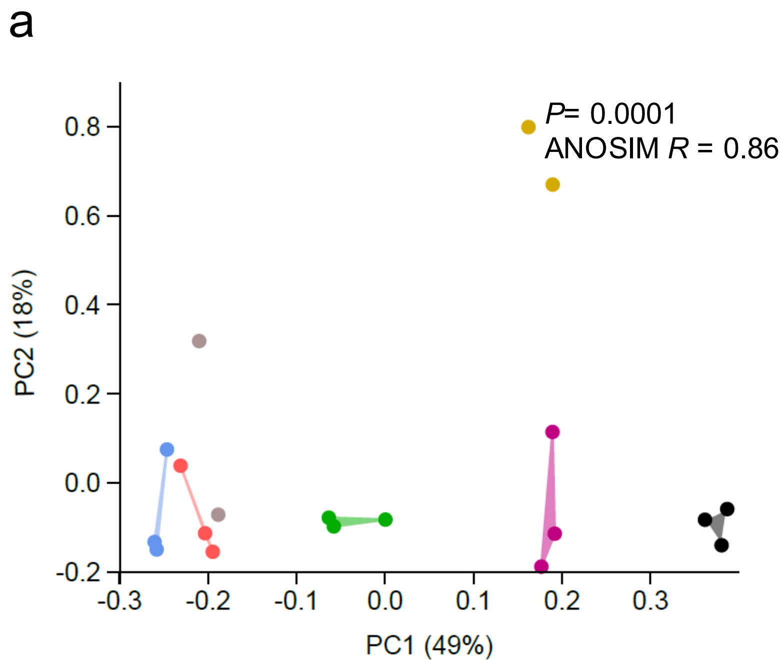
a
P= 0.0001
ANOSIM R = 0.86
PC2 (18%)
PC1 (49%)

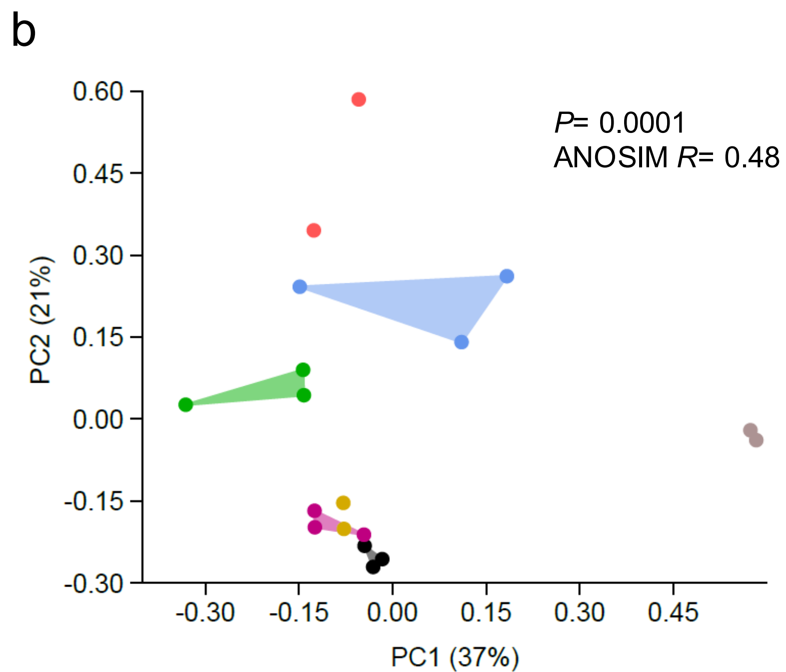
b
P= 0.0001
ANOSIM R= 0.48
PC2 (21%)
PC1 (37%)

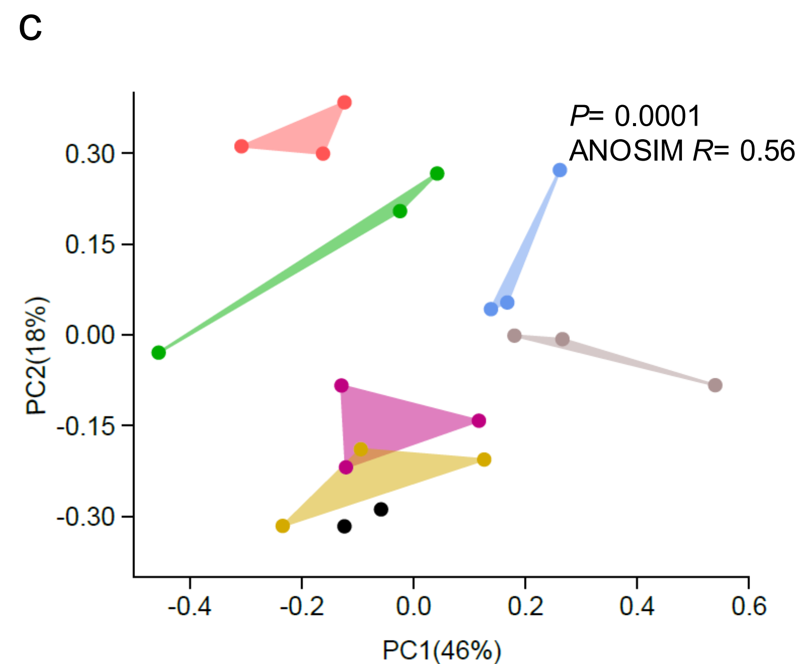
c
P= 0.0001
ANOSIM R= 0.56
PC2(18%)
PC1(46%)

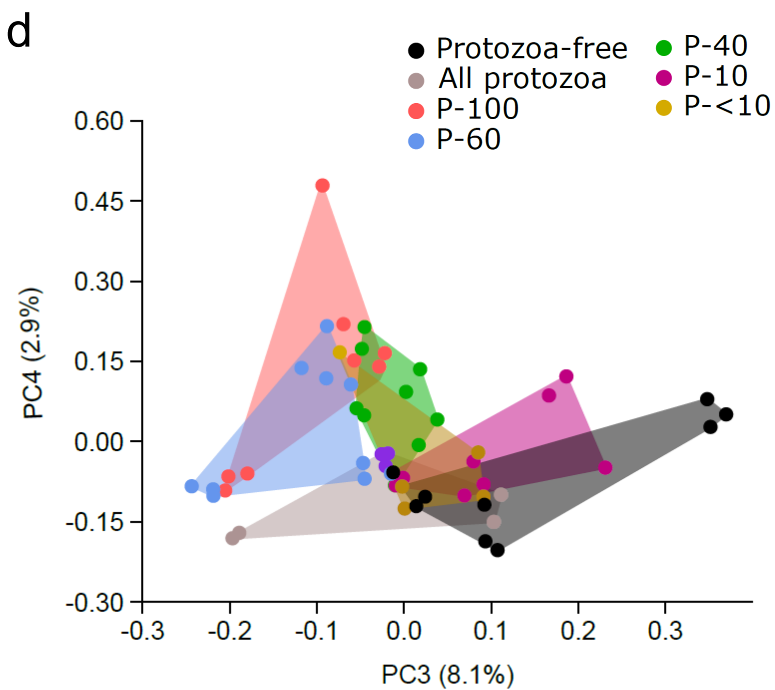
d
Protozoa-free
All protozoa
P-100
P-60
P-40
P-10
P-<10
PC4 (2.9%)
PC3 (8.1%)

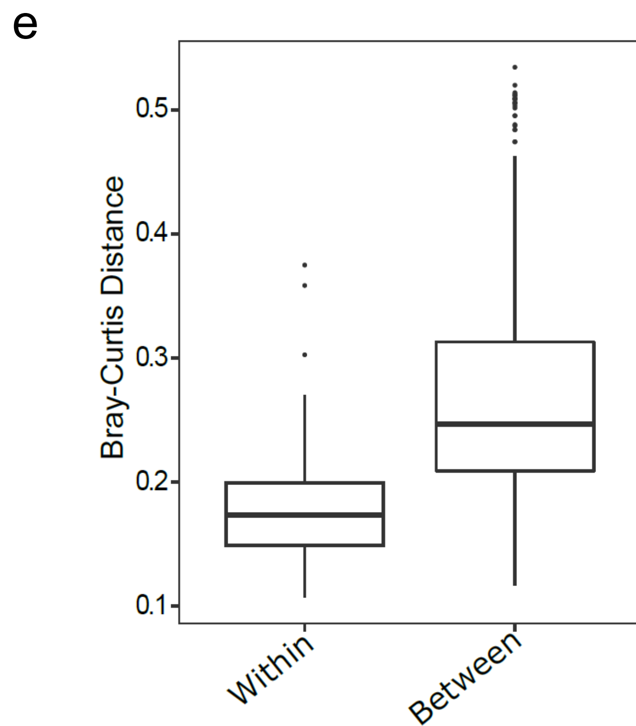
e
Bray-Curtis Distance
Within
Between

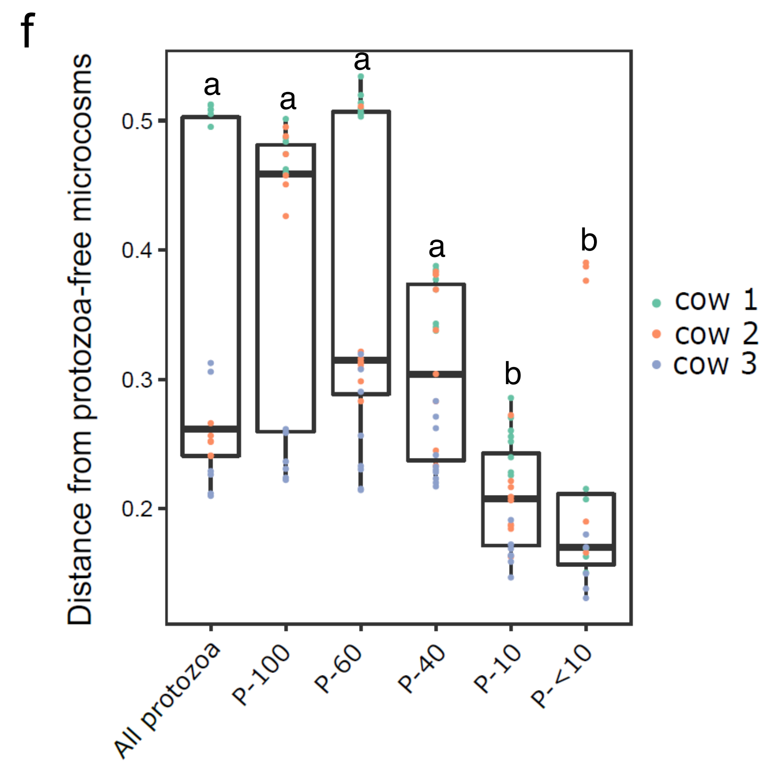
f
Distance from protozoa-free microcosms
All protozoa
P-100
P-60
P-40
P-10
P-<10
cow 1
cow 2
cow 3

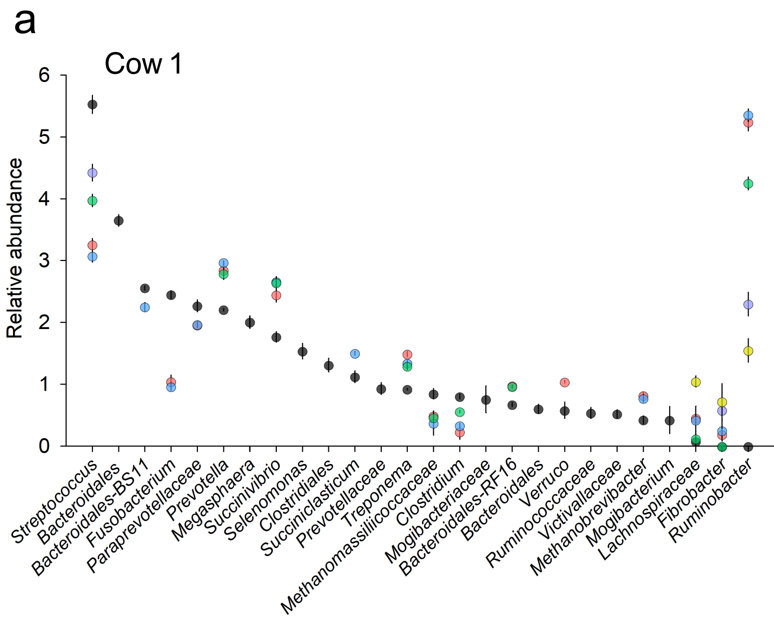

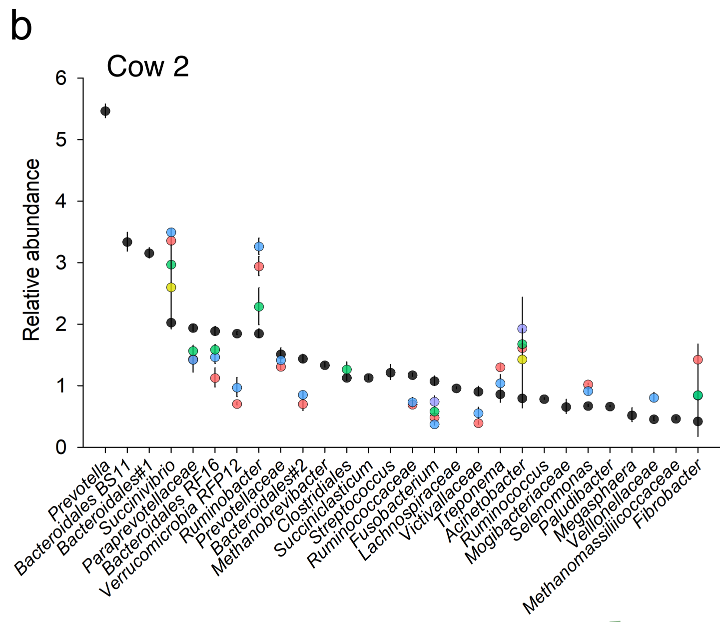

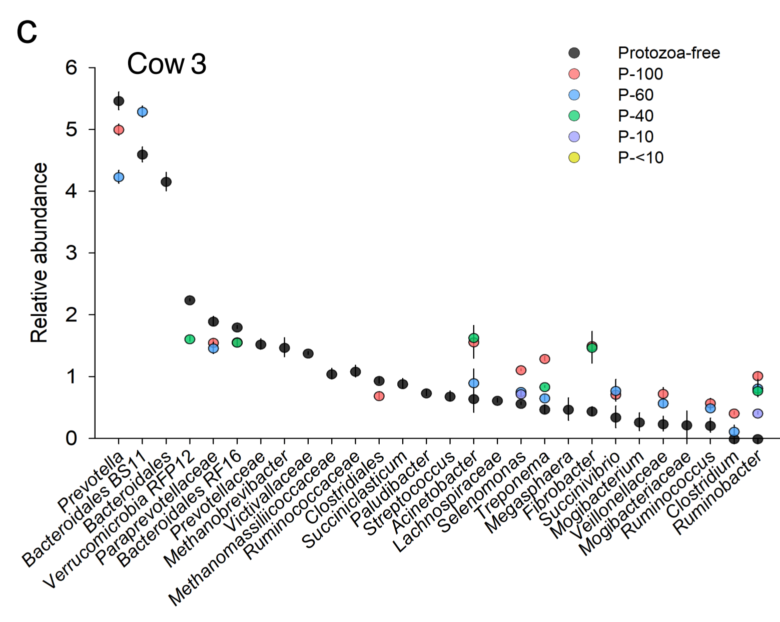

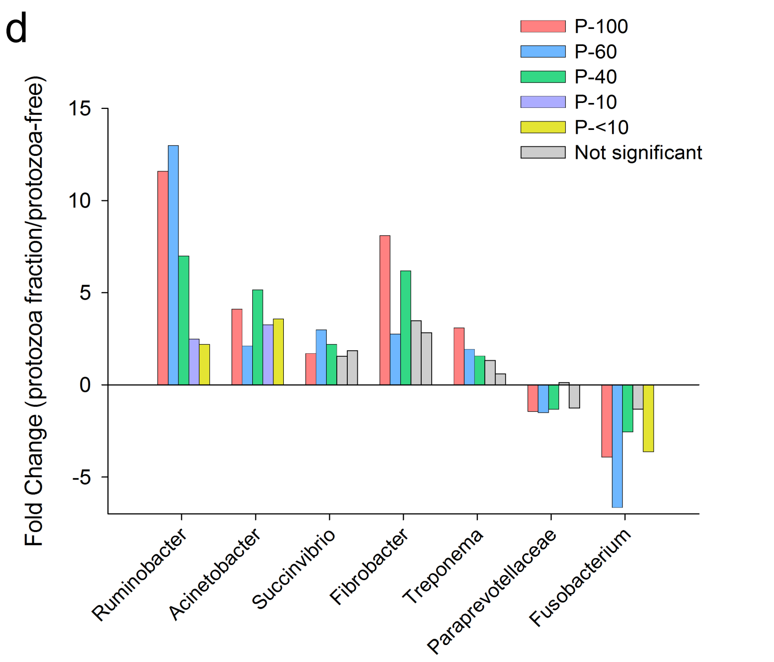

e

Phylum
Bacteroidetes
firmicutes
Verrucomicrobia
Proteobacteria
Spirochetes
Fibrobacteres
Fusobacteria
Lentisphera
Chlorflexi

Increase
Decrease
No change

Abundance
Protozoa-free
P-100
P-60
P-40